Enthalpy of Formation of the Cyclohexadienyl Radical and the C−H Bond Enthalpy of 1,4-Cyclohexadiene: An Experimental and Computational Re-Evaluation

Yide Gao, Nathan J. DeYonker, E. Chauncey Garrett III, Angela K. Wilson,* Thomas R. Cundari,* and Paul Marshall*

The Department of Chemistry, Center for Advanced Scientific Computing and Modeling (CASCaM), University of North Texas, 1155 Union Circle No. 305070, Denton, Texas 76203-5017

Received: February 12, 2009; Revised Manuscript Received: May 13, 2009

A quantitative understanding of the thermochemistry of cyclohexadienyl radical and 1,4-cyclohexadiene is beneficial for diverse areas of chemistry. Given the interest in these two species, it is surprising that more detailed thermodynamic data concerning the homolytic C−H bond enthalpies of such entities have not been forthcoming. We thus undertook an experimental and computational evaluation of (a) the enthalpy of formation of cyclohexadienyl radical (C_6H_7), (b) the homolytic C−H bond enthalpy of 1,4-cyclohexadiene (C_6H_8), and (c) the enthalpy of the addition of a hydrogen atom to benzene. Using laser photolysis experiments coupled with highly accurate ab initio quantum mechanical techniques, a newly recommended enthalpy of formation for C_6H_7 is determined to be 208.0 ± 3.9 kJ mol^{-1}, leading to a homolytic bond dissociation enthalpy of 321.7 ± 2.9 kJ mol^{-1}, almost 9 kJ mol^{-1} higher than previously determined enthalpies that used less certain experimental values for the C_6H_7 enthalpy of formation.

Introduction

The cyclohexadienyl radical (C_6H_7) is produced in a broad range of chemical applications. In their classic review more than 25 years ago, McMillen and Golden[1] stated, "As a prototypical radical of probable importance in the pyrolysis of certain aromatic systems... the cyclohexadienyl radical stability should be verified." 1,4-Cyclohexadiene and other compounds with weak bisallylic C−H bonds also serve as popular substrates in experimental studies of catalysts that homolytically activate C−H bonds;[2−6] C_6H_7 is thus an important intermediate in such catalytic processes.[2,3] Cyclohexadienyl and related radicals have also been suggested as intermediates in Bergman cyclizations.[7,8] Finally, radical C−H bond activation of bisallylic substrates is relevant to autoxidation and biomass utilization of polyunsaturated fatty acids (e.g., linoleic acid is a major component of soybean and cottonseed oils),[9,10] as well as the mechanism of lipoxygenase.[11]

The homolytic bond dissociation enthalpy (BDE) of the bisallylic C−H bond of 1,4-cyclohexadiene is far from certain. For example, recent catalysis-oriented papers report very different C−H homolytic BDEs for 1,4-cyclohexadiene. Feng et al. quote a C−H BDE for 1,4-cyclohexadiene of 305 ± 8 kJ mol^{-1} in a study of C−H activation by Ru complexes,[2] a value obtained from photoacoustic calorimetry (PAC) experiments.[12] Eckert et al.[3] quote a value of 318 kJ mol^{-1}, which is derived from multiple experiments.[13−16] Tallman et al. estimate a C−H bond enthalpy for 1,4-cyclohexadiene of 313 kJ mol^{-1} from kinetics experiments, calculations, and reaction rate/C−H BDE correlations.[9] Agapito et al.[17] review the pertinent literature vis-à-vis uncertainties in the thermochemistry of allylic moieties, including 1,4-cyclohexadiene. They measure an experimental BDE of 312.8 ± 6.1 kJ mol^{-1} from time-resolved PAC, while also theoretically obtaining a value of 326.3 kJ mol^{-1} for the bisallylic C−H bond of 1,4-cyclohexadiene via extrapolation of semiempirically scaled valence CCSD(T) energies.[18] Given the chemical importance of bisallylic moieties and the pentadienyl radicals derived from them, we thus undertook a combined experimental and computational evaluation of the enthalpy of formation of the cyclohexadienyl radical (C_6H_7).

At moderate temperatures the dominant pathway for the reaction of atomic hydrogen with benzene is addition to form cyclohexadienyl radicals:

$$H + C_6H_6\,(+M) \rightarrow C_6H_7\,(+M) \qquad (1)$$

where M is a bath gas molecule which collisionally stabilizes excited intermediates. C_6H_7 has been observed as a product of reaction 1 via its UV spectrum.[19,20] There have been several prior experimental investigations of the rate constant k_1 for reaction 1 below 800 K,[19−25] which have been critically reviewed by Baulch et al.[26] They based their recommendation on the work of Nicovich and Ravishankara.[21] However, Mebel et al. have since suggested that secondary chemistry could have been important under the conditions employed.[27] One measurement has appeared subsequently by Triebert et al.[28] Here we reinvestigate reaction 1 and its reverse, reaction −1,

$$C_6H_7\,(+M) \rightarrow H + C_6H_6\,(+M) \qquad (-1)$$

by the laser flash-photolysis/resonance fluorescence (LP-RF) technique and use the ratio of the rate constants to derive the equilibrium constant for reaction 1 and thus its thermochemistry.

Computational Methods

To complement the experiments, the $\Delta_f H^\circ_{298.15}$ of C_6H_7 was computed with a density functional (B3LYP) method, as well as with the G3B3 model chemistry,[29] the G3B3(MP2)-RAD model chemistry developed by Radom and coauthors,[30] the correlation-consistent composite approach (ccCA)[31−33] devel-

* To whom correspondence should be addressed. E-mail: akwilson@unt.edu (A.K.W.); t@unt.edu (T.R.C.); marshall@unt.edu (P.M.).

10.1021/jp901314y CCC: $40.75 © 2009 American Chemical Society
Published on Web 06/02/2009

oped in our laboratories, and a CCSD(T)-based method using extrapolations to the complete basis set limit. A formulation of ccCA using restricted open-shell wave functions (ROHF-ccCA) was also tested.[34] DFT computations and UHF reference ab initio computations were carried out with the Gaussian 03 software package.[35] All computations using an ROHF reference were carried out using Molpro 2006.1.[36] The ccCA methodology[31−33] is as follows.

For ccCA, structures were optimized at the B3LYP level of theory with the cc-pVTZ basis sets. Harmonic vibrational frequencies scaled by a factor of 0.9854 were also computed using B3LYP/cc-pVTZ at the equilibrium geometries to obtain the required zero-point vibrational energies (ZPVEs) and temperature-dependent enthalpy corrections. Single-point MP2 energies are extrapolated to the CBS limit using both a three-point mixed exponential/Gaussian formula

$$E(x) = E_{\mathrm{CBS}} + B\exp[-(x-1)] + C\exp[-(x-1)^2]$$

where x = D, T, or Q, and is the cardinal number or "ζ level" of the aug-cc-pVxZ basis sets, and the two-point (TQ) Schwartz inverse-power formula

$$E(l_{\max}) = E_{\mathrm{CBS}} + \frac{B}{\left(l_{\max}+\frac{1}{2}\right)^4}$$

where $l_{\max}$ is the maximum angular momentum of the basis set (equivalent to x for first- and second-row atoms and molecules). These two MP2 CBS energies are then averaged. Additive corrections to the MP2 energies to account for higher order electron correlation, core−valence correlation, and treatment of scalar relativistic effects were then made using the standard ccCA formalism in ref 33. For "ROHF-ccCA", the same ccCA approach was used, but with ROHF wave functions.[34] In all CCSD(T)/cc-pVTZ ccCA computations, the "RHF-UCCSD(T)" approach is used.[37]

For the "CBS-CCSD(T)" model chemistry, UQCISD/6-311G(d,p) theory implemented within Gaussian 03 was used to obtain equilibrium geometries and harmonic vibrational frequencies. Then single-point RHF-UCCSD(T) energies were derived using cc-pVTZ and cc-pVQZ basis sets and extrapolated to the infinite basis set limit using a two-point scheme based on the relation of Halkier et al.:[38]

$$E(x) = E_{\mathrm{CBS}} + \frac{B}{{l_{\max}}^3}$$

Zero-point vibrational energies and thermal corrections $H_{298} - H_0$ were based on the UQCISD frequencies scaled by 0.954. The harmonic-oscillator rigid-rotor approximation was employed, with the exception of extra corrections to the zero-point energy and thermal terms for the torsional mode of ethyl (treated as a free rotor),[39] the out-of-plane bending mode in CH_3 (corrected for anharmonicity as detailed previously),[40] and the torsional mode of ethane (treated via the method of Pitzer and Gwinn).[41] Corrections for core−valence electron correlation at the CCSD(T) level and scalar relativistic effects at the CISD level were made using the cc-pwCVTZ basis sets.[42]

Experimental Method

The apparatus and general approach for kinetic studies of H atom reactions have been detailed elsewhere.[43−46] The photochemical reactor is a stainless steel six-way cross heated within an oven. Gas temperatures T in the reaction zone, where the arms of the reactor (i.d. = 2.2 cm) intersect, are monitored with a retractable thermocouple corrected for radiation errors. Liquid benzene (Sigma-Aldrich, ≥99.9%) was degassed via two freeze−pump−thaw cycles at 77 K and then distilled twice from room temperature, in which the middle 80% portion was trapped at 77 K. Argon (Air Liquide, 99.9999%) was used as supplied. Mixtures of benzene vapor diluted in argon were prepared manometrically in glass bulbs, and the pressure was monitored with a capacitance manometer checked against a mercury barometer. The uncertainty in pressure is estimated as $\sigma \approx 0.5-1\%$ depending on the value. Mass-flow controllers, calibrated against a bubble meter, set the flows of dilute benzene and pure argon into the reactor. Around 5% of the argon purged regions in front of the optical windows of the reaction cell. The balance of the argon was premixed with the benzene dilution before entering the reactor. Other purposes of the argon bath gas are to quench excited species following the photolysis pulse, to ensure isothermal conditions during the reaction, and to slow diffusion of reactive species to the walls of the reactor.

Atomic hydrogen was generated by pulsed laser photolysis of a small fraction of benzene at 193 nm. An estimate of the initial concentration $[H]_0$ was obtained by combining the laser pulse energy F (corrected for reflection at the entrance window), the beam diameter of 1.0 cm, an estimated quantum yield of 0.77, and an absorption cross section of 5×10^{-17} cm^2 molecule^{-1},[47,48] which we took to be temperature-independent. We allowed for attenuation of the actinic radiation in the side arm, path length ∼11 cm, by the reactant before the radiation reaches the reaction zone. The yield of 0.77 was derived by comparing signals from photolysis of benzene and ammonia back-to-back at 296 K and 140 mbar of total pressure, corrected for attenuation of the probe beam and of the signal by absorption by the precursor at 121.6 nm. For these attenuation corrections we assumed an average concentration in the side arms of half of the bulk in the reaction zone. This is a crude approximation, so the uncertainty in the yield of H from benzene is at least a factor of 2. The H atoms are monitored by time-resolved resonance fluorescence at 121.6 nm, excited by a microwave-powered resonance lamp through which flowed a 0.1% dilution of H_2 in Ar. Magnesium fluoride optics were employed, together with a dry air filter and an interference filter (Acton, centered at 122 nm, fwhm = 8 nm) to isolate Lyman α signals from any light emission from the aromatic molecules. The H atom fluorescence, plus a constant background from scattered light, was observed with a solar-blind photomultiplier tube operated in a photon counting mode, and signals from typically 200−8000 pulses were accumulated in a multichannel scaler. The total signal I_f below 500 K decayed exponentially after the photolysis pulse and was fit as a function of time t to the form

$$I_f = A\exp(-k_{ps1}t) + B$$

where B is the constant background and k_{ps1} is an effective pseudo-first-order decay coefficient. An example time profile is shown in the inset to Figure 1. Photolysis pulses were repeated at ca. 2 Hz, which allowed for fresh mixtures to enter the reaction zone between pulses. The average residence time of the gas in the heated reactor before photolysis, τ_{res}, was varied to check for any effects arising from mixing or thermal decomposition.

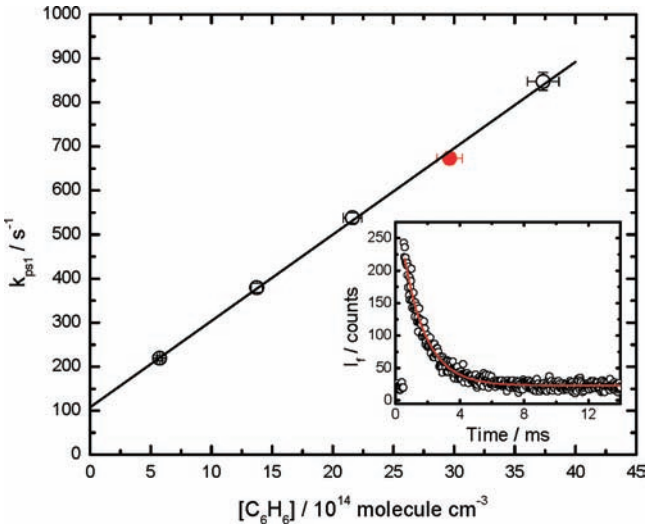

Figure 1. Example of a plot of pseudo-first-order decay coefficient k_{ps1} for H atoms vs benzene concentration at 339 K, a total pressure of 143 mbar, and a photolysis pulse energy of 0.25 mJ. The inset shows the exponential decay of the fluorescence signal I_f corresponding to the filled point.

Below 500 K the mechanism is

$$H + C_6H_6 \rightarrow C_6H_7$$

$$H \rightarrow \text{loss}$$

Experiments were conducted under the pseudo-first-order condition $[C_6H_6] \gg [H]_0$, so that we may write

$$d[H]/dt = -k_1[H][C_6H_6] - k_{diff}[H] = -k_{ps1}[H]$$

where k_{diff} accounts for loss of H atoms other than by reaction with C_6H_6, mainly through diffusion. The observation that k_{diff} was smaller at higher pressures at each given temperature (see Table 1) supports this assignment, although there may also be contributions from secondary reactions of H with other species present. We therefore expect an exponential decay of [H] as $[H]_0 \exp(-k_{ps1}t)$. A weighted linear plot[49] of k_{ps1} vs $[C_6H_6]$ yields k_1 as the slope, and an example is shown in Figure 1. At higher temperatures formation of C_6H_7 becomes reversible, so that the mechanism now includes dissociation, reaction -1, with a first-order rate constant k_{-1} and

$$C_6H_7 \rightarrow \text{loss}$$

which allows for loss of C_6H_7 by processes that do not regenerate H atoms, which may include diffusion, the cyclohexadienyl self-reaction, or reaction with species such as C_6H_5. This loss step is assigned an effective first-order rate constant k_{loss}. The corresponding rate law is

$$[H] = [H]_0[(\lambda_1 + k_{-1} + k_{loss})e^{\lambda_1 t} - (\lambda_2 + k_{-1} + k_{loss})e^{\lambda_2 t}]/(\lambda_1 - \lambda_2)$$

where, with $k' = k_1[C_6H_6]$, λ_1 and λ_2 are defined as

$$2\lambda_{1,2} = -(k' + k_{diff} + k_{-1} + k_{loss}) \pm [(k' + k_{diff} + k_{-1} + k_{loss})^2 - 4(k'k_{loss} + k_{diff}k_{-1} + k_{loss}k_{diff})]^{1/2}$$

This rate law implies a biexponential decay, and an example is shown in logarithmic form as the inset in Figure 2. Before the fluorescence signal was fitted, the background as measured from pretrigger information was subtracted, and then the [H] profile was fit according to the above equations with a fixed loss rate k_{diff} for atomic H and the other three rate constants allowed to vary. Variation of k' in the fits to the biexponential decays indicated that the data allowed for changes of up to about 10% in k'. The value of k_{diff} was chosen iteratively to make the intercept of a plot of k' vs $[C_6H_6]$ (see Figure 2) equal to zero. The slope of this plot equals k_1.

Experimental Results

The experimental conditions and results are summarized in Table 1. Typically five or six reactant concentrations were employed at each set of conditions to determine k_1, and the maximum values are given in the tables. The corresponding approximate values of the initial [H] are also shown, which indicate that benzene was in excess by at least a factor of 100 and confirm that pseudo-first-order conditions were attained. Below 400 K the k_1 values for reaction 1 exhibited a consistent increase with increasing photolysis energy F, revealing an influence from secondary chemistry involving photolysis or reaction products. Accordingly, these data below 400 K were linearly extrapolated to $F = 0$, as shown in Figure 3. At 416 K the rate constant for the target reaction is an order of magnitude higher than at 298 K, so that even though the $[C_6H_6]$ employed was smaller by factors around 2−3 than at the lower temperatures, the pseudo-first-order consumption of H atoms in reaction 1 was faster by roughly a factor of 3, which helps isolate the target from secondary chemistry. This secondary chemistry might involve C_6H_5 and/or C_6H_7 radicals, and we speculate that as the temperature is raised these species may be scavenged more rapidly by processes other than reaction with H. Because above 400 K we observe independence of the k_1 results from F and $[H]_0$, they were combined at each temperature as the weighted mean, calculated via the method of Bevington.[50] No consistent influence of pressure or residence was observed, which indicates negligible effects from decomposition or mixing.

Above 500 K kinetic data were extracted from the more complicated mechanism involving reversible formation of cyclohexadienyl radicals. Table 1 gives information about the reverse rate constant k_{-1} as well as the loss rate for the adduct other than by dissociation back to reactants, k_{loss}. For each run, it was verified that the addition rate was proportional to the benzene concentration and that the dissociation rate assigned to the adduct was independent of the benzene concentration, as seen in Figure 2. As noted above, k_{loss} might reflect reaction of cyclohexadienyl with phenyl or other species formed in the system. Its nature is unknown, but because it is larger than k_{diff} for the much faster moving H atoms, diffusional loss is not the major factor. We do note that k_{loss} is apparently independent of $[C_6H_6]$ (see Figure 2 for an example). Support for the mechanisms employed here comes from the consistent fit through both the low- and high-temperature data seen when the k_1 results are plotted in

TABLE 1: Summary of Rate Constant Measurements for H + C_6H_6[a]

T, K	τ_{res}, s	F, mJ	PD,[b] 10^{14} photons cm^{-2}	P, mbar	$[C_6H_6]_{max}$, 10^{15} molecules cm^{-3}	$[H]_{0,max}$, 10^{13} molecules cm^{-3}	$k_1 \pm \sigma_{k_1}$, 10^{-13} cm^3 molecule^{-1} s^{-1}	$k_{-1} \pm \sigma_{k_{-1}}$, s^{-1}	$k_{loss} \pm \sigma_{k_{loss}}$, s^{-1}	k_{diff}, s^{-1}	K_c, 10^{-15} cm^3 molecule^{-1}	K_{eq}, 10^4
297	3.2	0.58	2.8	73	3.41 ± 0.10	3.4	1.81 ± 0.09			86		
297	3.2	0.32	1.5	73	3.41 ± 0.10	1.9	1.15 ± 0.01			98		
297	3.2	0.23	1.1	73	3.41 ± 0.10	1.3	0.95 ± 0.02			93		
297	3.2	0.16	0.8	73	3.41 ± 0.10	0.9	0.79 ± 0.02			96		
298	6.3	0.41	1.6	147	4.15 ± 0.12	2.3	1.41 ± 0.01			63		
298	6.3	0.27	1.1	147	4.15 ± 0.12	1.5	1.13 ± 0.03			55		
298	6.3	0.16	0.6	147	4.15 ± 0.12	0.9	0.82 ± 0.03			57		
298	3.2	0.33	0.6	73	7.11 ± 0.21	1.3	0.99 ± 0.02			99		
298	3.2	0.24	0.4	73	7.11 ± 0.21	1.0	0.87 ± 0.02			101		
298	3.2	0.13	0.2	73	7.11 ± 0.21	0.5	0.70 ± 0.02			96		
298							0.37 ± 0.02[c]					
339	5.5	0.37	1.6	143	3.73 ± 0.11	2.1	2.20 ± 0.03			130		
339	5.5	0.25	1.1	143	3.73 ± 0.11	1.5	1.96 ± 0.03			108		
339	5.5	0.19	0.8	143	3.73 ± 0.11	1.1	1.67 ± 0.04			109		
340	2.8	0.38	1.3	73	4.55 ± 0.14	2.1	2.15 ± 0.03			154		
340	2.8	0.26	0.9	73	4.55 ± 0.14	1.4	1.84 ± 0.04			144		
340	2.8	0.19	0.7	73	4.55 ± 0.14	1.1	1.68 ± 0.04			126		
340							1.22 ± 0.05[c]					
416	4.6	0.49	3.6	144	1.88 ± 0.06	2.5	3.66 ± 0.13			150		
417	2.2	0.15	0.8	71	2.87 ± 0.09	0.9	3.68 ± 0.21			197		
416							3.67 ± 0.11[d]					
510	1.8	0.09	0.5	72	3.04 ± 0.09	0.5	9.54 ± 0.29	83 ± 15	90 ± 45	206		
510	1.8	0.20	1.1	72	3.04 ± 0.09	1.2	8.90 ± 0.38	88 ± 26	82 ± 24	190		
510							9.30 ± 0.23[d]	84 ± 13[d]			11.1 ± 1.7	15.8 ± 2.4
521	1.8	0.32	3.3	71	0.69 ± 0.02	0.9	11.0 ± 1.5	173 ± 12	54 ± 23	251		
521	3.5	0.19	1.1	144	2.67 ± 0.08	1.1	9.73 ± 0.43	133 ± 24	70 ± 8	183		
521	3.5	0.08	0.5	144	2.67 ± 0.08	0.5	10.2 ± 0.9	182 ± 64	87 ± 27	195		
522	1.9	0.36	3.5	76	0.87 ± 0.03	1.1	9.58 ± 0.43	136 ± 9	129 ± 20	266		
521							9.90 ± 0.37[d]	148 ± 7[d]			6.7 ± 0.4	9.3 ± 0.6
529	3.5	0.47	3.6	147	1.72 ± 0.05	2.3	13.5 ± 1.1	159 ± 13	126 ± 21	181		
530	3.4	0.20	1.5	141	1.87 ± 0.06	1.0	13.0 ± 0.3	186 ± 11	113 ± 26	183		
530	3.4	0.10	0.7	141	1.87 ± 0.06	0.5	12.9 ± 0.6	221 ± 44	105 ± 27	155		
530	3.4	0.78	6.4	141	1.47 ± 0.04	3.5	11.9 ± 0.4	151 ± 11	162 ± 41	200		
530	1.4	0.45	3.2	71	2.03 ± 0.06	2.4	12.4 ± 0.9	178 ± 18	150 ± 32	299		
530							12.7 ± 0.2[d]	169 ± 6[d]			7.5 ± 0.3	10.2 ± 0.4
540	1.7	0.52	4.3	71	1.45 ± 0.04	2.3	13.6 ± 1.2	226 ± 18	199 ± 25	345		
540	1.7	0.32	2.7	71	1.45 ± 0.04	1.4	12.1 ± 1.0	276 ± 48	165 ± 28	317		
541	1.7	0.06	0.4	72	2.35 ± 0.07	0.3	10.8 ± 0.5	336 ± 42	122 ± 24	322		
541	1.7	0.15	1.0	72	2.35 ± 0.07	0.8	10.2 ± 0.6	304 ± 19	131 ± 30	305		
541							11.0 ± 0.3[d]	270 ± 12[d]			4.1 ± 0.2	5.5 ± 0.3
550	3.3	0.19	1.4	143	2.01 ± 0.06	1.0	14.1 ± 0.4	397 ± 49	158 ± 21	150		
550	3.3	0.08	0.6	143	2.01 ± 0.06	0.4	13.9 ± 0.5	532 ± 47	123 ± 18	196		
552	3.4	0.40	4.1	144	0.72 ± 0.02	1.1	15.7 ± 0.7	276 ± 29	153 ± 19	165		
551							14.3 ± 0.3[d]	357 ± 22[d]			4.0 ± 0.3	5.3 ± 0.4
559	1.7	0.24	1.7	73	2.01 ± 0.06	1.3	13.6 ± 0.7	491 ± 16	182 ± 14	276		
559	1.7	0.08	0.6	73	2.01 ± 0.06	0.4	12.2 ± 1.1	625 ± 43	158 ± 6	302		
560	3.2	0.16	1.4	137	1.31 ± 0.04	0.7	13.4 ± 1.0	507 ± 107	162 ± 21	151		
559							13.3 ± 0.5[d]	507 ± 15[d]			2.6 ± 0.1	3.4 ± 0.1
571	1.7	0.35	3.0	76	1.38 ± 0.04	1.5	14.9 ± 0.5	556 ± 60	227 ± 8	348		
573	1.6	0.14	1.0	71	1.84 ± 0.06	0.7	12.9 ± 0.8	851 ± 91	192 ± 8	373		
573	1.6	0.30	2.2	71	1.84 ± 0.06	1.5	14.2 ± 0.7	632 ± 31	238 ± 15	356		
574	3.3	0.16	1.1	145	2.17 ± 0.07	0.9	14.1 ± 0.9	843 ± 241	213 ± 38	172		
573							14.4 ± 0.3[d]	638 ± 26[d]			2.3 ± 0.1	2.9 ± 0.1
581	3.2	0.57	3.6	145	2.40 ± 0.07	3.2	15.6 ± 0.7	723 ± 77	311 ± 74	186		
581	3.2	0.26	1.7	145	2.40 ± 0.07	1.4	14.2 ± 0.7	1016 ± 167	239 ± 30	135		
581	1.6	0.12	0.6	144	3.08 ± 0.09	0.7	15.1 ± 0.5	920 ± 114	146 ± 28	146		
582	1.6	0.41	2.7	72	2.25 ± 0.07	2.2	18.7 ± 0.5	712 ± 127	309 ± 40	334		
582	1.6	0.90	6.0	72	2.25 ± 0.07	4.9	17.9 ± 0.9	669 ± 136	311 ± 96	353		
582	1.7	0.33	2.3	76	2.09 ± 0.06	1.8	13.0 ± 0.4	1036 ± 177	226 ± 31	312		
582	1.7	0.13	0.9	76	2.09 ± 0.06	0.7	12.4 ± 0.8	1154 ± 325	183 ± 24	309		
582							14.9 ± 0.2[d]	805 ± 48[d]			1.9 ± 0.1	2.4 ± 0.1

[a] Errors are statistical only. [b] Photon density at the center of the reaction zone. [c] From linear extrapolation to $F = 0$. [d] Weighted mean value.

Arrhenius form in Figure 4. These data may be summarized as

$$k_1 = (6.8 \pm 1.0) \times 10^{-11} \exp((-18.2 \pm 0.6\ \text{kJ mol}^{-1})/RT)\ \text{cm}^3\ \text{molecule}^{-1}\ \text{s}^{-1}$$

over 297−582 K, where the uncertainties represent 1 standard deviation for the Arrhenius parameters.

Consideration of these along with the covariance leads to purely statistical 1σ uncertainties in the fit of 4−11% in k_1. Combination in quadrature with an allowance of 5% for possible systematic errors in the pressure and temperature leads to an overall 95% confidence interval of 22%. The present k_1 data are in excellent accord with the results of Nicovich and Ravishankara[21] below 500 K (see Figure 4), and the greatest difference is less than 5%. The 298 K value of Triebert et al.[28] of $(5.6 \pm 2.8) \times 10^{-14}$ cm^3 molecule^{-1} s^{-1} is also in agreement. This latter measurement extends the pressure range for the bath gas down to 4 mbar of He, so reaction 1 does appear to be at the high-pressure limit under our conditions, as argued previously by Nicovich and Ravishankara.[21] In the temperature range

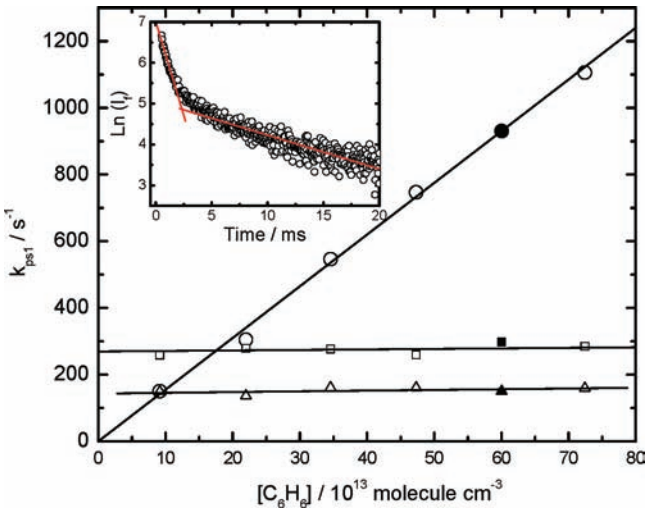

Figure 2. First-order rates vs benzene concentration in the equilibrium regime at 552 K, a 144 mbar total pressure, and a photolysis pulse energy of 0.40 mJ: circles, k' for addition to C_6H_6; squares, k_{-1} for dissociation of C_6H_7 to H + C_6H_6; triangles, k_{loss} for loss of C_6H_7 by other processes. The inset shows a biexponential decay of the H atom fluorescence signal corresponding to the filled points, plotted logarithmically.

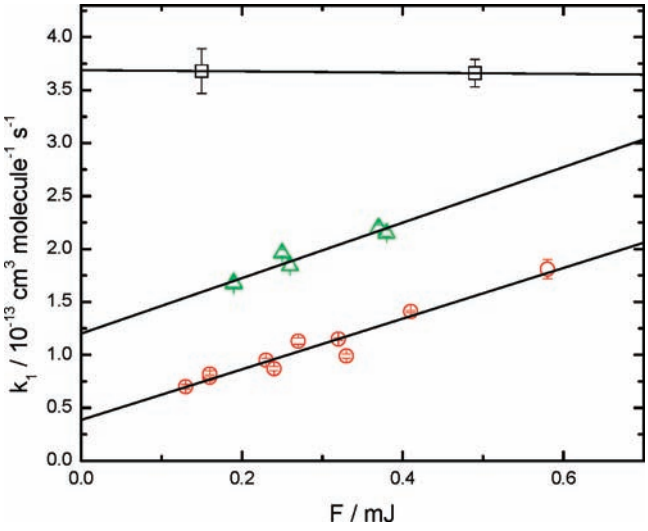

Figure 3. Observed rate constant for H + C_6H_6 as a function of laser photolysis energy F at three temperatures, with extrapolations to zero energy at 298 and 340 K.

515−570 K the previously reported values are in the range (5−9) × 10^{-14} cm^3 molecule s^{-1}.[21] These are an order of magnitude smaller than our values or what would be expected from simple linear extrapolation of the lower temperature Arrhenius plot. We analyzed the published biexponential decay (Figure 2 of ref 21) obtained at 515 K and, with both forward and reverse rate constants as adjustable parameters, obtained k_1 = 1.0 × 10^{-12} cm^3 molecule^{-1} s^{-1}. This is in good accord with our results and the extrapolation of either data set from low temperatures (see Figure 4), but not the previously tabulated values of k_1.[21] This fit, with k_{diff} fixed at 50 s^{-1}, also yielded k_{loss} = 16 s^{-1} and k_{-1} = 74 s^{-1}. This latter value agrees with the published expression.[21]

Kinetic data for the dissociation of cyclohexadienyl, reaction −1, which varies strongly with temperature, are only available by the present method in the narrow temperature window where the time scale is comparable to that for addition. Our results are shown in Figure 5, along with those of Nicovich and

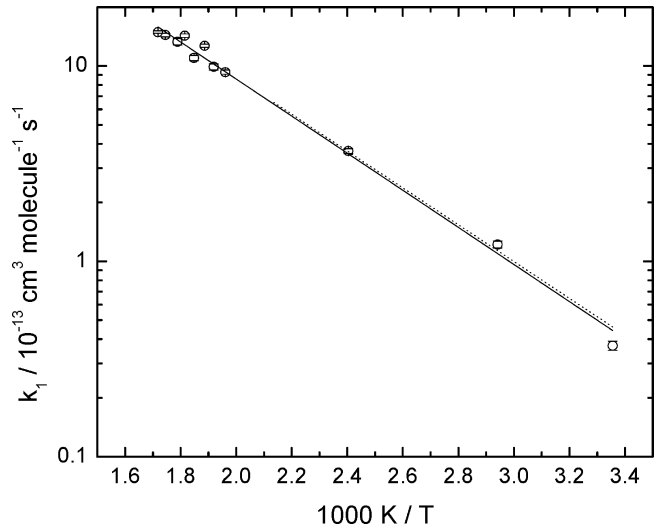

Figure 4. Arrhenius plot of rate constant k_1 for H + C_6H_6 → C_6H_7: circles and solid line, present work and fit; dotted line, fit from Nicovich and Ravishankara.[21]

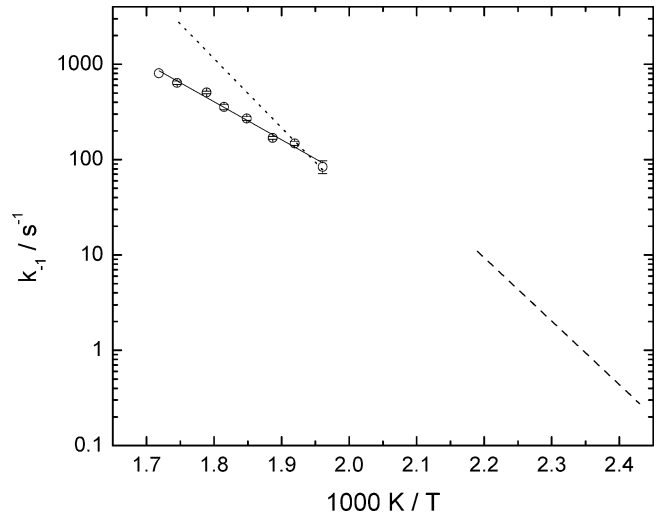

Figure 5. Arrhenius plot of rate constant k_{-1} for C_6H_7 → H + C_6H_6: circles and solid line, present work and fit; dotted line, fit from Nicovich and Ravishankara;[21] dashed line, analysis of Tsang.[51]

Ravishankara.[21] It may be seen that there are discrepancies of up to a factor of 4 with the high-temperature end of the present work, even though the measurements were made by a similar method and interpreted in terms of the same mechanism and rate law.[21] An Arrhenius fit of our results over 510−580 K is

$$k_{-1} = (6.0^{+5.6}_{-2.9}) \times 10^9 \exp((-76.3 \pm 3.0\ \text{kJ mol}^{-1})/RT)\ \text{s}^{-1}$$

where the errors are ±1σ and are purely statistical. Together with the covariance, they imply 95% statistical error limits of 20%. We note that, unlike k_{-1} itself, because of the short temperature range, the individual Arrhenius parameters are not well-defined as may be demonstrated as follows. Tsang[51] has combined relative rate data from James and Stuart[52] with measurements of the cyclohexadienyl self-reaction by Sauer and Ward,[19] and these data are also included in Figure 5. An Arrhenius fit through the middle of this data set and ours implies k_{-1} values that deviate from the fit expression above by at most ±20%, but yields very different Arrhenius parameters of A = 1.2 × 10^{11} s^{-1} and E_a = 90 kJ mol^{-1}.

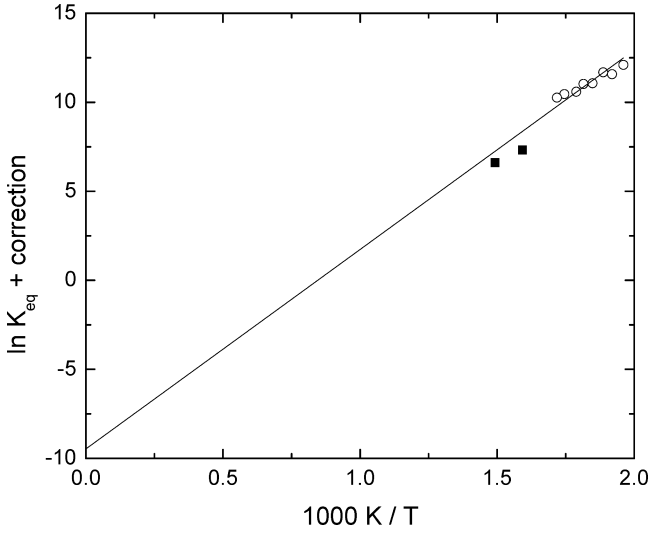

Figure 6. van't Hoff plot for $H + C_6H_6 \rightleftarrows C_6H_7$: open circles, present work; solid squares, Berho et al.[20]

These kinetics for the reverse reaction can be used to obtain the equilibrium constant for reaction 1 and thus thermodynamic information about the cyclohexadienyl radical. At each temperature the ratio k_1/k_{-1} is the concentration equilibrium constant K_c, which is listed in Table 1. With a standard state of 10^5 Pa, this is converted to the thermodynamic equilibrium constant K_{eq}, i.e., the ratio of the activity of the product divided by the activities of the reactants. A van't Hoff plot of ln K_{eq} vs $1/T$ should have a slope equal to $-\Delta H/R$ and an intercept of $\Delta S/R$. Addition of a minor correction x to ln K_{eq} of

$$x = \frac{\Delta S_{298} - \Delta S_T}{R} + \frac{\Delta H_T - \Delta H_{298}}{RT}$$

accounts for the temperature dependence of S and H and is based on heat capacities derived from UQCISD/6-311G(d,p) data. We find $x(T) = (6.9 \times 10^{-7})T^2 + (8.1 \times 10^{-5})T - 0.09$ over 298−800 K, and it is around 0.2 at the temperatures of interest.

A "third-law" analysis is shown in Figure 6, where the intercept is constrained by an ab initio $\Delta S_{298} = -78.7$ J K^{-1} mol^{-1}, based on the harmonic-oscillator rigid-rotor assumption and UQCISD/6-311G(d,p) data (see the Supporting Information). For comparison, the empirical analysis of Tsang[51] corresponds to $\Delta S_{298} = -82.7$ J K^{-1} mol^{-1}, while the density functional and BAC-MP4 results of Berho et al.[20] were summarized as $\Delta S_{298} = -80.5 \pm 4.0$ J K^{-1} mol^{-1}. These error limits allowed for uncertainties in the lowest frequency modes. We adopt this same uncertainty here. We also allow for errors of up to a factor of 2 in K_{eq}. Taken in quadrature, these two error sources propagate to a ±3.9 kJ mol^{-1} error limit for $\Delta_f H^\circ_{298.15}$, which was found here to be −92.9 kJ mol^{-1}. This is the negative of the C_6H_6−H bond dissociation enthalpy. The corresponding fit is seen in Figure 6 to be reasonably close to the two equilibrium values derived by Berho et al.,[20] to within 1 natural logarithm unit, or a factor of 2.7. They studied perturbation by benzene of [H] profiles in the Cl_2/H_2 chain reaction, at higher temperatures where reaction 1 is equilibrated rapidly and their kinetic modeling was insensitive to the separate values of k_1 and k_{-1}.

An alternative "second-law" analysis does not constrain the intercept and leads to $\Delta S_{298} = -21$ J K^{-1} mol^{-1} and $\Delta_f H^\circ_{298.15} = 62$ kJ mol^{-1}. The error limits on these unreasonable values are very large however, because the $1/T$ interval is small: for example, the same factor of 2 uncertainty in K_{eq} yields error limits of 34 kJ mol^{-1} for $\Delta_f H^\circ_{298.15}$. We therefore focus on the third-law results. The corresponding enthalpy of formation ($\Delta_f H^\circ_{298.15}$) for C_6H_7 from the third-law bond dissociation enthalpy, using experimental values for H and C_6H_6,[53] is $\Delta_f H^\circ_{298.15} = 208.0 \pm 3.9$ kJ mol^{-1}. The value measured here for $\Delta_f H^\circ_{298.15}(C_6H_7)$ can be compared to those of previous reports. For example, Berho et al.[20] report a comparable value, but with considerably less precision: 212 ± 12 kJ mol^{-1}. Tsang[51] derived a very similar value of $\Delta_f H^\circ_{300} = 209 \pm 5$ kJ mol^{-1} by combining the Nicovich−Ravishankara results with other data. As indicated by several authors,[17,20,51] earlier values of the $\Delta_f H^\circ_{298.15}$ of cyclohexadienyl spanned a range of more than 25 kJ mol^{-1}.

SCHEME 1: Isodesmic Reaction Used To Compute the $\Delta_f H^\circ_{298.15}$ Value of Cyclohexadienyl Radical

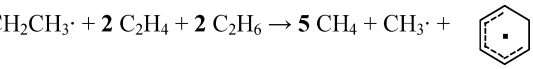

SCHEME 2: Direct Addition Reaction Used To Compute the $\Delta_f H^\circ_{298.15}$ Value of Cyclohexadienyl Radical

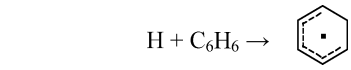

Theoretical Results

The computed $\Delta_f H^\circ_{298.15}$ of the cyclohexadienyl radical was obtained via two methods: (a) an isodesmic reaction (Scheme 1) using experimentally known $\Delta_f H^\circ_{298.15}$ values[53] for the smaller molecules and (b) a direct addition of hydrogen atom to benzene (Scheme 2). The latter more closely corresponds with the experimental measurements performed as part of the present research. A table of the experimental values obtained from the Third Millennium Ideal Gas and Condensed phase Thermochemical Database for Combustion with Updates from Active Thermochemical Tables (report TAE 960, Table 4),[53] as well as the molecular energies obtained via the various levels of theory and composite methods are given as Supporting Information.

It is generally known that isodesmic-type reaction schemes successfully allow for cancellation of errors from ab initio methods, especially compared to the determination of enthalpies of formation via atomization energies.[54] Beyond isodesmic reactions, a host of reaction schemes have been developed that use increasingly larger chemical fragments that better model the local environment of the constituent atoms. Recently, Wheeler, Allen, and co-workers have examined these reaction schemes and defined a hierarchy of essentially convergent fragmentation reactions for closed-shell hydrocarbons.[55] While they suggest a practical scheme for homodesmotic and hyper-homodesmotic radical reactions, there may be many ways of constructing such reactions. Using conventions of closed-shell organic reactions, our predicted "homodesmotic" and "hyper-homodesmotic" $\Delta_f H^\circ_{298.15}$ values for cyclohexadienyl differed from those of the isodesmic approaches by up to 17.6 kJ mol^{-1}! This is mainly due to the increased uncertainty in experimental enthalpies of formation for larger hydrocarbon radicals, generally 1−2 orders of magnitude larger than those of the smaller molecular fragments utilized in our isodesmic reactions for C_6H_7. Coupled with large uncertainties in the experimental enthalpies of formation of larger radical species, open-shell reaction schemes pose a significant problem. For now, the isodesmic reactions are the best compromise, and a more systematic

TABLE 2: Standard Enthalpies of Formation of Cyclohexadienyl Radical at 298.15 K from Various Levels of Theory and Experiment

method	isodesmic $\Delta_f H^\circ_{298.15}$ (kJ mol^{-1})	direct addition $\Delta_f H^\circ_{298.15}$ (kJ mol^{-1})
B3LYP/cc-pVTZ	208.2	218.0
G3B3	207.4	223.1
G3B3(MP2)-RAD	207.1	213.5
ccCA	214.8	213.6
ROHF-ccCA	208.8	206.6
CBS-CCSD(T)	208.3	208.8
exptl	212 ± 12[a]	
	209 ± 5[b]	
exptl (this work)	208.0 ± 3.9	

[a] Reference 20. [b] Reference 52.

TABLE 3: BDEs of Cyclohexadienyl To Form Hydrogen Atom + C_6H_6 and 1,4-Cyclohexadiene To Form Hydrogen Atom + C_6H_7 (kJ mol^{-1}) at 298.15 K

method	C_6H_7 BDE	1,4-cyclohexadiene BDE	1,4-cyclohexadiene BDE (av)
B3LYP/cc-pVTZ	82.9	331.2 (321.4)[a]	326.3
G3B3	77.8	336.3 (320.6)	328.4
G3B3(MP2)-RAD	87.4	326.7 (320.3)	323.5
ccCA	87.3	326.8 (328.0)	327.4
ROHF-ccCA	94.3	319.8 (322.0)	320.9
CBS-CCSD(T)	92.1	322.0 (321.5)	321.7
exptl		312.8 ± 6.1[b]	
exptl (this work)	92.9 ± 3.9		

[a] The first value listed is obtained via Scheme 2 (direct addition), while the value in parentheses is via Scheme 1 (isodesmic reactions). The average of these two values is given in the last column. [b] Reference 17.

assessment of homodesmotic radical reactions is currently under way in our laboratories.

Table 2 shows the enthalpy of formation of cyclohexadienyl radical at each level of theory. Using an isodesmic reaction (Scheme 1), all methods except for the UHF-based ccCA are within the experimental error bars of both the study of Tsang[51] and the experimental value obtained in this study. The $\langle S^2 \rangle$ value of cyclohexadienyl radical within the various single-point energy steps of a UHF-based ccCA is 1.15−1.17, while the $\langle S^2 \rangle$ values in the various G3B3 steps are 1.16−1.20, significantly higher than the optimal doublet expectation value of 0.75. This highlights the importance of considering spin contamination for radical thermochemistry.

When the direct addition reaction (Scheme 2) is used to compute the theoretical $\Delta_f H^\circ_{298.15}$ value for cyclohexadienyl radical, there is no fortuitous cancellation of errors from spin contamination in both products and reactants. Surprisingly, there are no obvious trends from comparison of UHF-based versus ROHF-based versions of G3 and ccCA. The UHF-based ccCA enthalpies of formation are overestimated using both an isodesmic and a direct addition thermochemical cycle, but the ROHF-based ccCA shows good agreement regardless of which scheme is employed to extract the $\Delta_f H^\circ_{298.15}$ of C_6H_7. On the other hand, both G3B3 and G3B3(MP2)-RAD give reasonable values via Scheme 2 and rather overestimated values using an isodesmic reaction, Scheme 1. The ROHF-ccCA and CBS-CCSD(T) model chemistries are the only two methods that agree with the laser photolysis value using both thermochemical cycles.

Via Scheme 2, the newly measured experimental bond dissociation enthalpy for cyclohexadienyl radical to form hydrogen and benzene is calculated and compared with a very high level of theory [CBS-CCSD(T) in Table 3]. The ROHF-ccCA method gives the only value for the BDE (94.3 kJ mol^{-1}) that closely matches the CBS-CCSD(T) calculation (92.1 kJ mol^{-1}). These two results are both within the experimental uncertainties quoted in this work. The G3B3(MP2)-RAD model chemistry, designed to give high-quality and extremely efficient energies for radical species, does not compare well to ccCA and CBS-CCSD(T) thermochemical values in this particular example.

Next, the BDE of 1,4-cyclohexadiene to hydrogen atom and cyclohexadienyl radical was computed (shown in Table 3) given the importance of this compound as a model substrate in catalysis and its relevance to areas such as lipid oxidation. This BDE is computed using the previously obtained $\Delta_f H^\circ_{298.15}$ values for C_6H_7 via both reaction schemes. Taking the average of both reaction schemes, the ROHF-ccCA and CBS-CCSD(T) levels of theory are in very good agreement, differing by only 0.8 kJ mol^{-1}, with the CBS-CCSD(T) method predicting an average BDE of 321.7 kJ mol^{-1} for the two thermochemical cycles. Using other levels of theory, the BDE is overestimated (Table 3). For example, the averaged B3LYP/cc-pVTZ bond dissociation enthalpy is 5.6 kJ mol^{-1} higher than the value obtained using CBS-CCSD(T), typical of DFT BDEs.[17,56] Note that only the CBS-CCSD(T) isodesmic results have been adjusted for specific anharmonic contributions in the methyl radical, ethyl radical, and ethane. Without these corrections, the $\Delta_f H^\circ_{298.15}$ of C_6H_7 is calculated to be 205.1 kJ mol^{-1}. Propagating this shift of −3.2 kJ mol^{-1} leads to a CBS-CCSD(T) 1,4-cyclohexadiene BDE value of 318.3 kJ mol^{-1}. Compared to the ROHF-ccCA C_6H_8 BDE of 319.8 kJ mol^{-1} (via Scheme 1), it is clear that the ROHF-ccCA isodesmic value benefits slightly from cancellation of errors. However, via Scheme 2, the ROHF-ccCA BDE is in very good agreement with CBS-CCSD(T) results.

To properly assess the accuracy of the ROHF-ccCA and CBS-CCSD(T) values, uncertainties for a broad range of isodesmic reaction schemes and BDEs must be defined. While the 2σ error of ccCA calibrated against the G3/99 training set is 10.9 kJ mol^{-1}, the statistical analysis is performed with the inclusion of enthalpies of formation calculated using an atomization energy scheme.[33] Wheeler, Allen, and coauthors have found an average error of 2.5 kJ mol^{-1} relative to their post-CCSD(T) "focal point" model chemistry values for the BDEs of 1,3-cyclohexadiene and cyclopentadiene using an isodesmic scheme with CCSD(T)/cc-pVTZ computations.[55] Post-CCSD(T) electron correlation effects often cancel and quickly converge to a "full-CI" limit once connected quadruple excitations are incorporated into the wave function. This has been observed for isogyric reaction energies of smaller hydrocarbons,[57] as well as for atomization energies and proton affinities of small molecules.[58,59] With the utilization of complete basis set energies, treatment of relativistic effects and core−valence effects, and including experimental uncertainties in the isodesmic scheme, we would expect ROHF-ccCA and the CBS-CCSD(T) values to have error bars no larger than this 2.5 kJ mol^{-1} error in quadrature with the error propagation of experimental uncertainties of reference compounds (equal to ∼1.5 kJ mol^{-1}; see the Supporting Information), which results in overall error bars of 2.9 kJ mol^{-1} for the isodesmic scheme. Even with such a conservative estimate of uncertainty, our ROHF-ccCA and CBS-CCSD(T) values (320.9 and 321.7 kJ mol^{-1}, respectively) lie at the upper range of values reported by Agapito et al.[18] (312.8 ± 6.1 kJ mol^{-1}). Agapito and coauthors recognize that their experimental value for the BDE of 1,4-cyclohexadiene is a lower limit, and our results support that conclusion.

Summary and Conclusions

In summary, laser photolysis experiments are coupled with high-level theory to provide accurate enthalpies of formation and bond dissociation enthalpies for cyclohexadienyl radical. Our new recommended value for the cyclohexadienyl radical $\Delta_f H^\circ_{298.15}$ is 208.0 ± 3.9 kJ mol^{-1}, and high-level computations accurately reproduce this result. The C_6H_7 enthalpy of formation is used in conjunction with a restricted open-shell formulation of ROHF-ccCA and a higher level coupled-cluster-based approach to give newly recommended BDEs for cyclohexadienyl radical (92.9 ± 3.9 kJ mol^{-1}) and 1,4-cyclohexadiene (321.7 ± 2.9 kJ mol^{-1}). Even via isodesmic reaction schemes that are designed to enhance cancellation of error, DFT and G*n* methods fail to give quantitatively acceptable results when compared to the very expensive and highly accurate CBS-CCSD(T) approach. It is clear that a coupled-cluster-based model chemistry (such as the CBS-CCSD(T) approach used in this study) will be intractable for bisallyl radicals that are substantially larger than cyclohexadienyl. Since results calculated using the ROHF-ccCA model chemistry were in very good agreement with those calculated using the CBS-CCSD(T) model chemistry, ccCA is a viable alternative for comparison and validation in tandem with high-quality experiments, or for computation of allyl radical thermochemistry when experimental information is unavailable. The calculated thermodynamics reported here plus the evidence of spin contamination (vide supra) makes it clear that an accurate energetic description of radicals, particularly conjugated organic radicals (and, parenthetically, likely most classes of open-shell transition-metal complexes), will require high-quality wave-function-based electron correlation formalisms that utilize restricted open-shell reference states.

Acknowledgment. CASCaM is supported by a grant from the U.S. Department of Energy (DOE) (BER-08ER64603). This work was partially supported by grants from the U.S. DOE, Basic Energy Sciences (DE-FG02-03ER15387; T.R.C.), National Science Foundation (CHE-0809762; A.K.W.), Welch Foundation (Grant B-1174; P.M.), and UNT Faculty Research Fund (P.M.). The computations employed UNT's NSF-CRIF computational chemistry resource (Grant CHE-0741936) and the UNT Research Cluster operated by UNT Academic Computing Services. E.C.G. was supported by the NSF-REU site in Chemistry at UNT (Grant CHE-0648843). We acknowledge Professor Wesley D. Allen for sharing results prior to publication.

Supporting Information Available: A table of the experimental enthalpies of formation (from ref 53) used and molecular energies using ccCA, G3B3, G3B3(MP2)-RAD, B3LYP cc-pVTZ, and CBS-CCSD(T). This material is available free of charge via the Internet at http://pubs.acs.org.

References and Notes

(1) McMillen, D. F.; Golden, D. M. *Annu. Rev. Phys. Chem.* **1982**, *33*, 493.
(2) Feng, Y.; Gunnoe, T. B.; Grimes, T. V.; Cundari, T. R. *Organometallics* **2006**, *25*, 5456.
(3) Eckert, N. A.; Vaddadi, S.; Stoian, S.; Lachicotte, R. J.; Cundari, T. R.; Holland, P. L. *Angew. Chem., Int. Ed.* **2006**, *45*, 6868.
(4) Fulton, J. R.; Sklenak, S.; Bouwkamp, M. W.; Bergman, R. G. *J. Am. Chem. Soc.* **2002**, *124*, 4722.
(5) Holland, A. W.; Bergman, R. G. *J. Am. Chem. Soc.* **2002**, *124*, 14684.
(6) Fox, D. J.; Bergman, R. G. *Organometallics* **2004**, *23*, 1656.
(7) Lockhart, T. P.; Comita, P. B.; Bergman, R. G. *J. Am. Chem. Soc.* **1981**, *103*, 4082.
(8) Lockhart, T. P.; Bergman, R. G. *J. Am. Chem. Soc.* **1981**, *103*, 4091.
(9) Tallman, K. A.; Roschek, B.; Porter, N. A. *J. Am. Chem. Soc.* **2004**, *126*, 9240.
(10) Corma, A.; Iborra, S.; Velty, A. *Chem. Rev.* **2007**, *107*, 2411.
(11) Goldsmith, C. R.; Jonas, R. T.; Stack, T. D. P. *J. Am. Chem. Soc.* **2002**, *124*, 83.
(12) Burkey, T. J.; Majewski, M.; Griller, D. *J. Am. Chem. Soc.* **1986**, *108*, 2218.
(13) Bordwell, F. G.; Cheng, J. P.; Harrelson, J. A. *J. Am. Chem. Soc.* **1988**, *110*, 1229.
(14) Bordwell, F. G.; Cheng, J.; Ji, G. Z.; Satish, A. V.; Zhang, X. *J. Am. Chem. Soc.* **1991**, *113*, 9790.
(15) Parker, V. D. *J. Am. Chem. Soc.* **1992**, *114*, 7458.
(16) Arends, I. W. C. E.; Mulder, P.; Clark, K. B.; Wayner, D. D. M. *J. Phys. Chem.* **1995**, *99*, 8182.
(17) Agapito, F.; Nunes, P. M.; Cabral, B. J. C.; dos Santos, R. M. B.; Simões, J. A. M. *J. Org. Chem.* **2007**, *72*, 8770.
(18) Truhlar, D. G. *Chem. Phys. Lett.* **1998**, *294*, 45.
(19) Sauer, M. C.; Ward, B. *J. Phys. Chem.* **1967**, *71*, 3971.
(20) Berho, F.; Rayez, M.-T.; Lesclaux, R. *J. Phys. Chem. A* **1999**, *103*, 5501.
(21) Nicovich, J. M.; Ravishankara, A. R. *J. Phys. Chem.* **1984**, *88*, 2534.
(22) Sauer, M. C.; Mani, I. *J. Phys. Chem.* **1970**, *74*, 59.
(23) Knutti, R.; Bühler, R. E. *Chem. Phys.* **1975**, *7*, 229.
(24) Louw, R.; Lucas, H. J. *Recl. Trav. Chim. Pays-Bas* **1973**, *922*, 55.
(25) Hoyermann, K.; Preuss, A. W.; Wagner, H. Gg. *Ber. Bunsen-Ges. Phys. Chem.* **1975**, *79*, 156.
(26) Baulch, D. L.; Cobos, C. J.; Cox, R. A.; Esser, C.; Frank, P.; Just, T.; Kerr, J. A.; Pilling, M. J.; Troe, J.; Walker, R. W.; Warnatz, J. *J. Phys. Chem. Ref. Data* **1992**, *21*, 411.
(27) Mebel, A. M.; Lin, M. C.; Yu, T.; Morokuma, K. *J. Phys. Chem. A* **1997**, *101*, 3189.
(28) Triebert, J.; Engelmann, L.; Olzmann, M.; Scherzer, K. *Z. Phys. Chem. (Muenchen)* **1998**, *205*, 33.
(29) Baboul, A. G.; Curtiss, L. A.; Redfern, P. C.; Raghavachari, K. *J. Chem. Phys.* **1999**, *110*, 7650.
(30) Henry, D. J.; Sullivan, M. B.; Radom, L. *J. Chem. Phys.* **2003**, *118*, 4849.
(31) DeYonker, N. J.; Cundari, T. R.; Wilson, A. K. *J. Chem. Phys.* **2006**, *124*, 114104.
(32) DeYonker, N. J.; Cundari, T. R.; Wilson, A. K.; Sood, C. A.; Magers, D. H. *J. Mol. Struct.: THEOCHEM* **2006**, *775*, 77.
(33) DeYonker, N. J.; Grimes, T.; Yockel, S.; Dinescu, A.; Mintz, B.; Cundari, T. R.; Wilson, A. K. *J. Chem. Phys.* **2006**, *125*, 104111.
(34) Williams, T. G.; DeYonker, N. J.; Ho, B. S. Cundari, T. R. Wilson, A. K. Manuscript in preparation.
(35) Frisch, M. J.; Trucks, G. W.; Schlegel, H. B.; Scuseria, G. E.; Robb, M. A.; Cheeseman, J. R.; Montgomery, J. A., Jr.; Vreven, T.; Kudin, K. N.; Burant, J. C.; Millam, J. M.; Iyengar, S. S.; Tomasi, J.; Barone, V.; Mennucci, B.; Cossi, M.; Scalmani, G.; Rega, N.; Petersson, G. A.; Nakatsuji, H.; Hada, M.; Ehara, M.; Toyota, K.; Fukuda, R.; Hasegawa, J.; Ishida, M.; Nakajima, T.; Honda, Y.; Kitao, O.; Nakai, H.; Klene, M.; Li, X.; Knox, J. E.; Hratchian, H. P.; Cross, J. B.; Bakken, V.; Adamo, C.; Jaramillo, J.; Gomperts, R.; Stratmann, R. E.; Yazyev, O.; Austin, A. J.; Cammi, R.; Pomelli, C.; Ochterski, J. W.; Ayala, P. Y.; Morokuma, K.; Voth, G. A.; Salvador, P.; Dannenberg, J. J.; Zakrzewski, V. G.; Dapprich, S.; Daniels, A. D.; Strain, M. C.; Farkas, O.; Malick, D. K.; Rabuck, A. D.; Raghavachari, K.; Foresman, J. B.; Ortiz, J. V.; Cui, Q.; Baboul, A. G.; Clifford, S.; Cioslowski, J.; Stefanov, B. B.; Liu, G.; Liashenko, A.; Piskorz, P.; Komaromi, I.; Martin, R. L.; Fox, D. J.; Keith, T.; Al-Laham, M. A.; Peng, C. Y.; Nanayakkara, A.; Challacombe, M.; Gill, P. M. W.; Johnson, B.; Chen, W.; Wong, M. W.; Gonzalez, C.; Pople, J. A. *Gaussian 03*, revision D.02; Gaussian, Inc.: Wallingford, CT, 2004.
(36) MOLPRO, version 2006.1, a package of ab initio programs: Werner, H.-J.; Knowles, P. J.; Lindh, R.; Manby, F. R.; Schütz, M.; Celani, P.; Korona, T.; Mitrushenkov, A.; Rauhut, G.; Adler, T. B.; Amos, R. D.; Bernhardsson, A.; Berning, A.; Cooper, D. L.; Deegan, M. J. O.; Dobbyn, A. J.; Eckert, F.; Goll, E.; Hampel, C.; Hetzer, G.; Hrenar, T.; Knizia, G.; Köppl, C.; Liu, Y.; Lloyd, A. W.; Mata, R. A.; May, A. J.; McNicholas, S. J.; Meyer, W.; Mura, M. E.; Nicklass, A.; Palmieri, P.; Pflüger, K.; Pitzer, R.; Reiher, M.; Schumann, U.; Stoll, H.; Stone, A. J.; Tarroni, R.; Thorsteinsson, T.; Wang, M. Wolf, A.; see http://www.molpro.net.
(37) Knowles, P. J.; Hampel, C.; Werner, H.-J. *J. Chem. Phys.* **1993**, *99*, 5219.
(38) Halkier, A.; Helgaker, T.; Jorgensen, P.; Klopper, W.; Koch, H.; Olsen, J.; Wilson, A. K. *Chem. Phys. Lett.* **1998**, *286*, 243.
(39) Marshall, P. *J. Phys. Chem. A* **1999**, *103*, 4560.
(40) Schwartz, M.; Peebles, L. R.; Berry, R. J.; Marshall, P. *J. Chem. Phys.* **2003**, *118*, 557.
(41) Pitzer, K. S.; Gwinn, W. D. *J. Chem. Phys.* **1942**, *10*, 428.
(42) Peterson, K. A.; Dunning, T. H., Jr. *J. Chem. Phys.* **2002**, *117*, 10548.

(43) Ding, L.; Marshall, P. *J. Phys. Chem.* **1992**, *96*, 2197.
(44) Goumri, A.; Yuan, W.-J.; Ding, L.; Shi, Y.; Marshall, P. *Chem. Phys.* **1993**, *177*, 233.
(45) Peng, J.; Hu, X.; Marshall, P. *J. Phys. Chem. A* **1999**, *103*, 5307.
(46) Alecu, I. M.; Gao, Y. D.; Hsieh, P. C.; Sand, J. P.; Ors, A.; McLeod, A.; Marshall, P. *J. Phys. Chem. A* **2007**, *111*, 3970.
(47) Pantos, E.; Philis, J.; Bolovinos, A. *J. Mol. Spectrosc.* **1978**, *72*, 36.
(48) Feng, R.; Cooper, G.; Brion, C. E. *J. Electron Spectrosc. Relat. Phenom.* **2002**, *123*, 199.
(49) Irvin, J. A.; Quickenden, T. I. *J. Chem. Educ.* **1983**, *60*, 711.
(50) Bevington, P. R. *Data Reduction and Error Analysis for the Physical Sciences*; McGraw-Hill: New York, 1969; p 88.
(51) Tsang, W. *J. Phys. Chem.* **1986**, *90*, 1152.
(52) James, D. G. L.; Stuart, R. D. *Trans. Faraday Soc.* **1968**, *64*, 2752.
(53) Burcat, A.; Ruscic̀, B. Ideal Gas Thermochemical Database with updates from Active Thermochemical Tables (ftp://ftp.technion.ac.il/pub/supported/aetdd/thermodynamics mirrored at http://garfield.chem.elte.hu/Burcat/burcat.html).
(54) Hehre, W. J.; Radom, L.; Pople, J. A.; Schleyer, P. v. R. *Ab Initio Molecular Orbital Theory*; John Wiley & Sons, Inc.: New York, 1986.
(55) Wheeler, S. E.; Houk, K. N.; Schleyer, P. v. R.; Allen, W. D. *J. Am. Chem. Soc.* **2009**, *131*, 2547.
(56) Do Couto, P. C.; Guedes, R. C.; Cabral, B. J. C.; Simões, J. A. M. *Int. J. Quantum Chem.* **2002**, *86*, 297.
(57) Simmonett, A. C.; Schaefer, H. F.; Allen, W. D. *J. Chem. Phys.* **2009**, *130*, 044301.
(58) Karton, A.; Taylor, P. R.; Martin, J. M. L. *J. Chem. Phys.* **2007**, *127*, 064104.
(59) Czakó, G.; Mátyus, E.; Simmonett, A. C.; Császár, A. G.; Schaefer, H. F.; Allen, W. D. *J. Chem. Theory Comput.* **2008**, *4*, 1220.

JP901314Y